

SYNTHESIS AND CONFORMATIONAL STUDIES OF 4-CARBAMOYL-1-[(2-HYDROXYETHOXY)-METHYL]-5-(METHYLAMINO)IMIDAZOLE AND DERIVATIVES AS NEW ACYCLONUCLEOSIDE ANALOGUES\*<sup>1</sup>

George I. Birnbaum<sup>2</sup>

Division of Biological Sciences, National Research Council of Canada,  
Ottawa, Ontario, Canada K1A 0R6

Erik De Clercq

Rega Institute for Medical Research, Katholieke Universiteit Leuven, B-3000  
Leuven, Belgium

Peter W. Hatfield and Morris J. Robins<sup>3</sup>

Department of Chemistry, University of Alberta, Edmonton, Alberta, Canada  
T6G 2G2

**Abstract** — Crystals of the title compound (**3**) belong to the orthorhombic space group  $Pbc2_1$ , with  $a = 8.718(1)$ ,  $b = 8.718(1)$ ,  $c = 18.351(2)$ ,  $c = 12.570(2)$  Å. The structure was determined by direct methods and refined by least squares to a final value of  $R = 0.048$ . Two independent molecules were found in the asymmetric unit, each in a different conformation. Infrared and  $^1H$  nmr spectral evidence was compatible with intramolecular hydrogen bonding of the  $NH_2$  group of the 4-carbamoyl function (to N3 in both crystallographically independent molecules). However, no evidence for defined conformations of the 5-methylamino group or the acyclic side chain at N1 was found in the solution studies.  $^1H$  nmr spectra of the 5-(N-acetyl-N-methylamino) derivatives (**5** and **6**) of **3** showed restricted rotation of the side chain. Conjugation of the 4-carbamoyl and 5-methylamino groups was apparent in the solid-state conformers and also from uv spectra of **5** and **6**. Biological evaluation of **3** and its 5-desmethyl analogue in viral infected, neoplastic, and normal control mammalian cell cultures showed no inhibitory or cytotoxic effects at the highest concentrations tested.

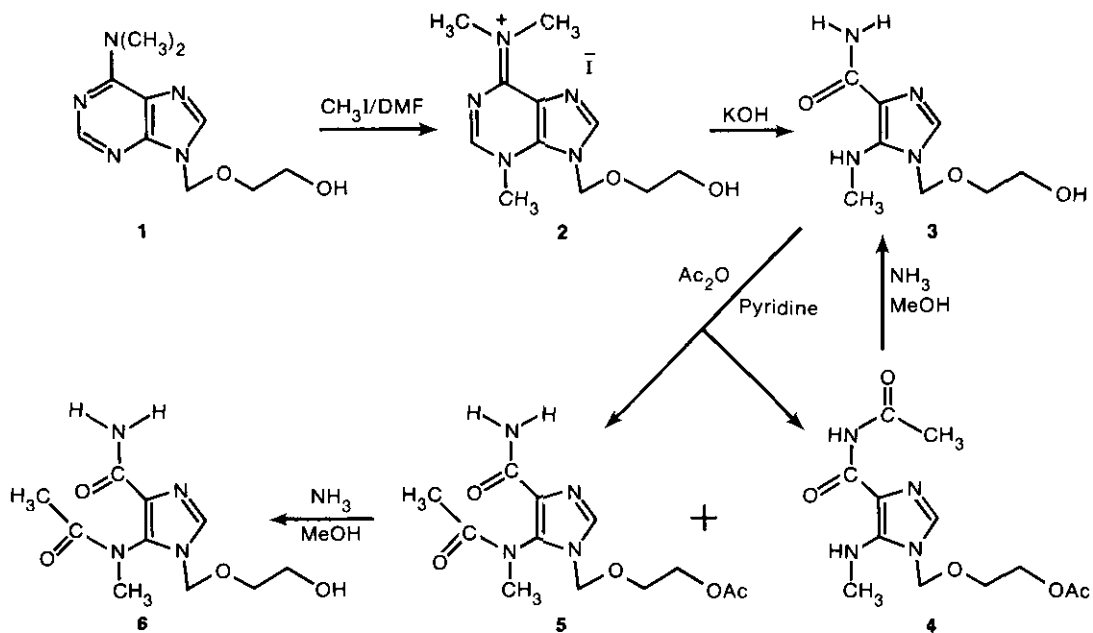
---

\* Dedicated to Prof. Gilbert Stork, on the occasion of his 65th birthday.

A dramatic recent advance in clinical antiviral chemotherapy has resulted from the discovery that 9-[(2-hydroxyethoxy)methyl]guanine (acyclovir) is phosphorylated quite efficiently by herpes simplex viral encoded thymidine kinase.<sup>4,5</sup> The resulting acyclovir monophosphate is converted to the di- and triphosphate levels by cellular host enzymes and the triphosphate is incorporated and complexed tightly at the genomic replication site by viral encoded DNA polymerases in infected cells.<sup>6</sup> Mammalian host thymidine kinases treat acyclovir as a far inferior substrate. A second therapeutic advantage results from the much lower incorporation by, and inhibition of, cellular DNA polymerases.<sup>7</sup> A large literature on acyclovir and related analogues has rapidly accumulated at the chemical, pharmacological and clinical levels.

Since the viral enzymes that normally catalyze phosphoryl transfer to O5' of the pyrimidine 2'-deoxynucleoside, thymidine, accept the somewhat remote 6-oxopurine analogue, acyclovir, as a substrate (while effectively rejecting the "thymine acyclonucleoside" analogue), it was of interest to evaluate an "imidazole acyclonucleoside" analogue with all of the elements of the purin-6-one ring in a flexible acyclic arrangement. Coupling methods are known to give N1 and N3 isomers of unsymmetrically substituted imidazoles.<sup>8,9</sup> Regiospecific synthesis of imidazole N1 isomers with the desired purine-type substituents can be accomplished by ring cleavage of appropriate purine precursors.<sup>10</sup>

Treatment of 9-[(2-hydroxyethoxy)methyl]-6-(dimethylamino)purine (1)<sup>11,12</sup> with methyl iodide in warm DMF resulted in formation of significant quantities of 3-methyl-6-(dimethylamino)purine in addition to the desired 9-[(2-hydroxyethoxy)methyl]-3-methyl-6-(dimethylamino)purine iodide (2)



salt. Glycosyl analogues of **2** are known to be thermally unstable presumably due to the "peri" repulsion of the crowded N3 and N9 substituents.<sup>13</sup>

Treatment of **1** with methyl iodide in DMF at -0°C for three weeks resulted in deposition of crystalline **2** in 55% yield. Aqueous ethanolic potassium hydroxide at reflux effected cleavage of the pyrimidine ring of **2** with loss of formate (C2) and dimethylamine to give **3** in 82% yield after purification.

X-ray crystallographic analysis of **3** showed the presence of two independent conformational isomers. Stereoscopic views of the two molecules, showing their overall conformation in the solid state and the atomic numbering scheme, are presented in Figure 1. Details of the molecular geometry are shown in Figure 2.

Imidazole moieties. In both molecules, the five atoms of the imidazole rings are coplanar; the maximum deviations from the mean planes are 0.005(3) Å in molecule A and 0.006(3) Å in molecule B. On the other hand, all atoms attached to the rings, except H2, are significantly displaced. The torsion angles about C4-C6 and C5-N9 (Fig. 2) indicate the extent to which the carboxamide and N-methyl groups are twisted from the imidazole rings.

Most equivalent bonds in the two molecules have the same lengths within experimental error. An exception are the values for C4-C5 which differ by 3.4σ. It is interesting that a review of C-C distances in imidazole groups revealed large fluctuations.<sup>14</sup> We compared the bond lengths to those in imidazole<sup>15</sup> and in three other imidazoles with a carboxamide group at C4 and a nitrogen substituent at C5, viz. AICA,<sup>16</sup> AICAR<sup>17</sup> and DTIC.<sup>18</sup> The C4-C5 bond is longer in molecule A than in any of the other molecules, but the difference is not significant when compared to AICA (1.380(7) Å) and AICAR (1.381(6) Å). All other bond lengths are in good agreement with those in the other substituted imidazoles. A comparison with unsubstituted imidazole should reveal the influence of the substituents at C4 and C5 on the electronic structure in the ring.

Table 1. Bond orders in imidazole rings.

Bond	mol. A	mol. B	imidazole
N1-C2	1.31	1.31	1.38
C2-N3	1.82	1.76	1.55
N3-C4	1.19	1.26	1.25
C4-C5	1.46	1.63	1.65
C5-N1	1.26	1.32	1.28

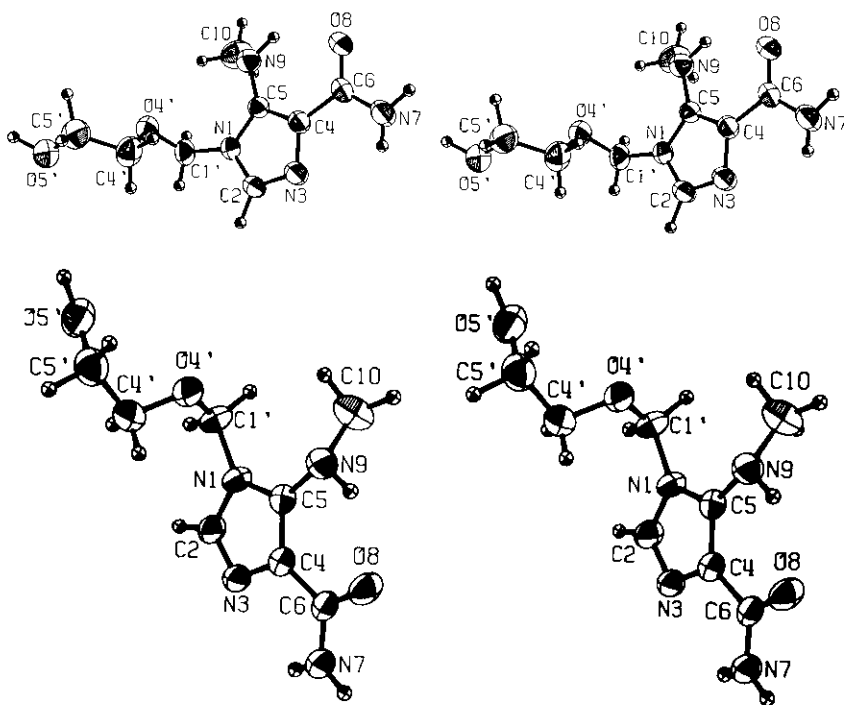


Fig. 1. Stereoscopic views of molecule A (top) and molecule B (bottom).

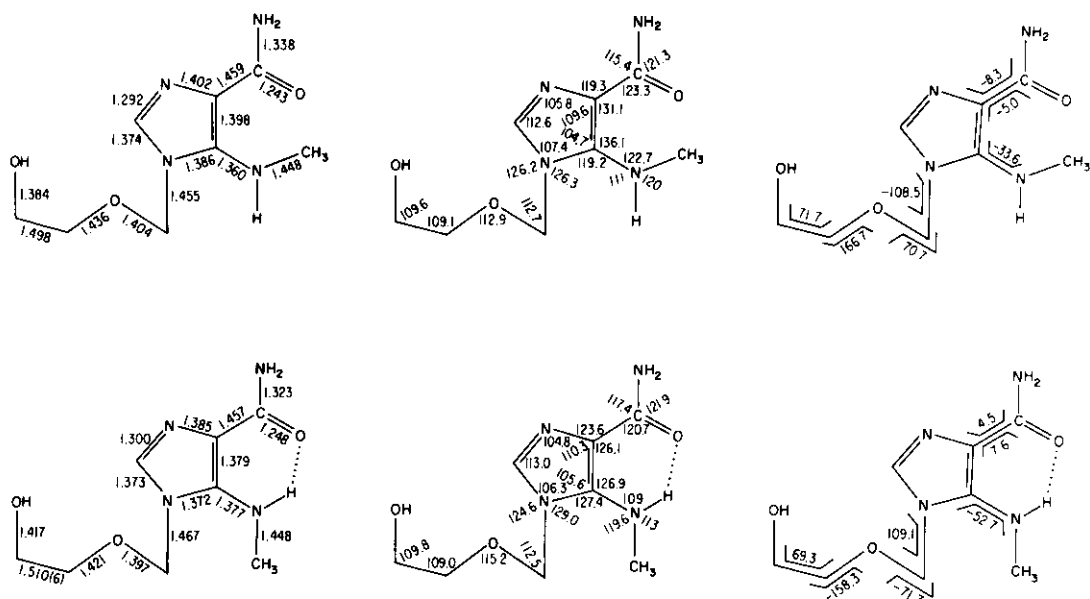


Fig. 2. Bond lengths (Å), bond angles, and torsion angles in molecules A (top) and B (bottom). Their estimated standard deviations are 0.003-0.005 Å and 0.2-0.3°, respectively.

Somewhat surprisingly, that influence is rather small. Each bond in imidazole is equal in length to at least one equivalent bond in the substituted imidazoles. The calculated bond orders<sup>19</sup> for each ring bond in the two molecules and in imidazole are listed in Table 1. The main difference can be seen in the C2-N3 bond. The sum of the bond orders is 7.04 for molecule A, 7.28 for molecule B, and 7.11 for imidazole.<sup>20</sup> Thus, it appears that the extent of electron donation by the N-CH<sub>3</sub> group into the ring is balanced by the withdrawal due to the -COHN<sub>2</sub> group. The bond orders for the C5-N9 bond are 1.38 and 1.30 in molecules A and B, respectively.

It should be noted that the carbamoyl group assumes the same conformation in both molecules, viz. with the C=O bond cis to C4-C5. This can be rationalized on steric grounds since in the alternate conformation (C-NH<sub>2</sub> cis to C4-C5) the distance between one of the amido-hydrogen atoms and one of the substituents at N9 would be too short. The observed conformation is further stabilized by an intramolecular hydrogen bond involving the amide group and N3. As a result, the carbamoylimidazole base shows some resemblance to adenine. In order to achieve antiviral activity it may be necessary to impose a change of this conformation, making the molecule resemble the antiherpes agent acyclovir.<sup>21</sup>

There are some small, but probably significant differences between the endocyclic angles in the two molecules. In molecule B, the angles at C4 and C5 are larger than in molecule A, while the angles at N1 and N3 are smaller. In view of this, and the fact that C4-C5 has more double bond character in molecule B (Table 1), one may conclude that C4 and C5 are more sp<sup>2</sup>-hybridized in molecule B.<sup>14</sup>

The differences between the other angles in the two molecules are very large and can be readily ascribed to the different conformations of the substituent at C5. In molecule A there is repulsion between O8 and the N-methyl group. The strain is relieved by pushing C10 away from the imidazole plane (the displacement amounts to 0.636(4) Å) and by widening the angles at C6, C4, C5 and N9. As a result, the angles C4-C6-N7, N3-C4-C6, and N1-C5-N9 are decreased. Despite these distortions, there is a short contact (2.19 Å, after normalizing C-H bonds to 1.09 Å) between O8 and one of the methyl hydrogen atoms. In contrast, there is an attractive interaction (hydrogen bond) between O8 and H9 in molecule B. Consequently, the endocyclic angles at C6, C4, C5 and N9 in this six-membered ring are much smaller than in molecule A, the difference between the two sums amounting to 30.5°. In fact, these angles are smaller than the corresponding ones in AICA<sup>16</sup> and in AICAR<sup>17</sup> in which the same intramolecular hydrogen bond was observed. The decrease of the C4-C5-N9 angle brings about a large increase of the N1-C5-N9 angle. This, and the larger C5-N1-C1' angle, serve to increase the distance between C10 and C1'.

Acyclo moieties. The conformations of the acyclic side chains are fairly similar in both molecules. The absolute values of the glycosidic torsion angles  $\chi_{CN}[C2-N1-C1'-O4']$  are the same,

molecule A with a negative  $\chi_{CN}$  being analogous to an  $\alpha$ -nucleoside and molecule B to a  $\beta$ -nucleoside. These torsion angles represent the preferred conformation of acyclonucleosides in which C1' is a disubstituted carbon atom; we recently calculated a mean value of  $96(12)^\circ$  for ten molecules.<sup>22</sup> The conformation about the C4'-C5' bond is gauche, in agreement with the well known gauche effect.<sup>23</sup> The overall conformation of the side chains is essentially the same as was observed in two of the three independent molecules of acyclovir.<sup>21</sup>

Most bond lengths are the same, within experimental error, in both molecules. The difference between the C5'-O5' bonds can be probably attributed to larger thermal motion in molecule A. As commonly observed in nucleosides, the C1'-O4' bonds are significantly shorter than the O4'-C4' bonds. All bond lengths are in very good agreement with those found in the same moiety in acyclovir.<sup>21</sup>

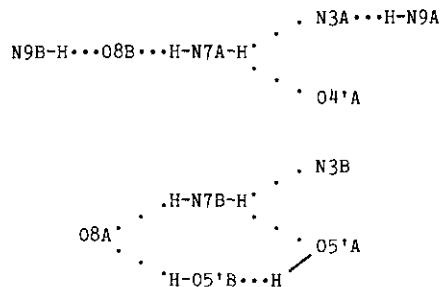
The bond angles also appear normal when compared to acyclovir. The wider angle at O4' in molecule B may be due to hydrogen bonding and packing requirements. In two molecules of a secoriboside the corresponding angles are  $119.4$  and  $117.5^\circ$ .<sup>24</sup>

Table 2. Distances and angles for hydrogen bonds.

<u>D</u>	<u>A</u>	<u>A at</u>	<u>Distances, Å</u>			<u>Angles, deg.</u>
			<u>D...A</u>	<u>H...A</u>	<u>H...A<sub>corr</sub></u>	<u>D-H...A</u>
N9B-H...O8B		$\underline{x}, \underline{y}, \underline{z}$	2.853(4)	2.06(6)	2.04	134
N7A-H71A...O8B		$1-\underline{x}, \underline{y}, \underline{1/2}+\underline{z}$	2.920(4)	2.01(6)	1.89	173
N7A-H72A...O4'A		$\underline{x}, \underline{1/2}-\underline{y}, \underline{1/2}+\underline{z}$	3.178(4)	2.43(5)	2.32	139
N7A-H72A...N3A		$\underline{x}, \underline{y}, \underline{z}$	2.724(4)	2.25(6)	2.21	109
N9A-H...N3A		$\underline{x}, \underline{1/2}-\underline{y}, \underline{-1/2}+\underline{z}$	3.379(4)	2.73(5)	2.51	141
N7B-H71B...O8A		$1-\underline{x}, \underline{y}, \underline{-1/2}+\underline{z}$	2.977(4)	2.05(4)	1.95	171
N7B-H72B...N3B		$\underline{x}, \underline{y}, \underline{z}$	2.834(4)	2.46(5)	2.40	108
N7B-H72B...O5'A		$\underline{x}, \underline{1/2}-\underline{y}, \underline{-1/2}+\underline{z}$	3.144(5)	2.41(5)	2.25	143
O5'A-H...O5'B		$\underline{x}, \underline{y}, \underline{z}$	2.852(4)	1.81(10)	2.04	140
O5'B-H...O8A		$1-\underline{x}, \underline{1/2}+\underline{y}, \underline{z}$	2.878(4)	2.01(8)	2.03	145

Hydrogen bonding and packing. Each molecule has four protons capable of participating in hydrogen bonds and all of them do, although, owing to steric hindrance, the interaction of H9A is quite weak and could be called electrostatic attraction rather than hydrogen bonding. The

intricate network formed by these bonds may be depicted schematically as follows:



The geometry of these bonds is given in Table 2. As commonly observed in X-ray analyses, the O-H and N-H bonds are not determined very accurately. By normalizing the covalent bond lengths to their nominal values of 0.97 and 1.04 Å, respectively, one obtains corrected H...A distances which reflect more accurately the strengths of these hydrogen bonds. Most of the bonds are fairly weak, either because of unfavourable geometry in intramolecular interactions or as a result of bifurcation.

Significant chemical shift differences between the two amide proton signals were observed in  $^1\text{H}$  nmr spectra of **3**. A larger shift magnitude was found in spectra determined in  $\text{CD}_3\text{CN}$  than in  $(\text{CD}_3)_2\text{SO}$  ( $\Delta\delta$   $\sim$ 0.64 ppm vs.  $\sim$ 0.16 ppm, respectively, at ambient conditions). These results are in harmony with resonance conjugation of the non-bonded electron pair of the amide nitrogen and intramolecular hydrogen bonding of the proximate N-H to N3. Competition by the electron-rich oxygen of  $(\text{CD}_3)_2\text{SO}$  would be expected to reduce the average lifetime and/or strength of the intramolecular N-H...N3 hydrogen bond relative to its environment in  $\text{CD}_3\text{CN}$  solution.

Infrared spectra of **3** in  $\text{CHCl}_3$  had intense carbonyl stretching bands at  $\sim$ 1645  $\text{cm}^{-1}$ , broad N-H stretching bands of low intensity at  $\sim$ 3330  $\text{cm}^{-1}$ , and two sharp N-H bands of higher intensity at  $\sim$ 3400 and  $\sim$ 3520  $\text{cm}^{-1}$ . The frequencies and relative intensities of these bands were essentially constant upon two- and four-fold dilutions.

No nmr solution evidence was obtained in support of the independent solid-state conformations in molecules A and B. The proton-decoupled 100.6 MHz  $^{13}\text{C}$  nmr spectrum of **3** in  $(\text{CD}_3)_2\text{SO}$  had a sharp singlet resonance at  $\delta$ 32.86 for the 5-NHCH<sub>3</sub> carbon that was generated as a single frequency output by the computer system. No twinning of proton frequencies was observed at 400 MHz under various conditions in several solvents. Irradiation at the resonance frequencies of the 5-NHCH<sub>3</sub> methyl protons or the imidazole H2 failed to produce significant difference NOE enhancements at other proton frequencies.

Spectra of solutions of **3** in  $\text{D}_2\text{O}$ ,  $\text{CD}_3\text{OD}$ ,  $(\text{CD}_3)_2\text{SO}$ , and  $\text{CD}_3\text{CN}$  at ambient conditions had differen-

tially shifted, but similar peak patterns for the nonexchangeable protons (except for the doublet to singlet peak change for  $\text{NHCH}_3$ , to  $\text{NDCH}_3$ ). Peak shapes for the AA'BB' spin system of the  $-\text{OCH}_2\text{CH}_2\text{O}-$  side chain fragment ranged from a "deceptively simple" apparent singlet for compound 2 in  $(\text{CD}_3)_2\text{SO}$  and compound 3 in  $\text{HCl}/\text{D}_2\text{O}/\text{CD}_3\text{CN}$  to apparent triplet/quartet patterns with additional splitting and lower intensity side-bands under various conditions. Irradiation at the hydroxyl proton triplet frequency of 3 in  $(\text{CD}_3)_2\text{SO}$  resulted in simplification of the lower field "apparent triplet" to a "distorted doublet" with a more nearly symmetrical form with respect to the upper field methyleneoxy multiplet.

Lowering the temperature of a solution of 3 in  $\text{CD}_3\text{CN}$  from  $35^\circ$  to  $25^\circ$  to  $0^\circ$  to  $-30^\circ\text{C}$  resulted in slight alterations of the peak shapes of the AA'BB' multiplets when expanded to 1 Hz/cm. The higher field methyleneoxy proton peak shifted to progressively higher fields relative to that of the lower, but the shifts were of the order of  $\Delta\delta$   $-0.1$  vs.  $-0.05$  ppm, respectively, over the  $+35^\circ$  to  $-30^\circ\text{C}$  extremes. The peaks from the H2,  $\text{NCH}_2\text{O}$ , and  $\text{NCH}_3$  protons remained at essentially constant shift values over this temperature range.

Similar temperature effects were observed with a solution of 3 in  $\text{CD}_3\text{OD}$ . At  $50^\circ\text{C}$ , the higher field AA'BB' multiplet was shifted downfield relative to the position of the corresponding apparent triplet at  $-20^\circ\text{C}$  and "broad singlet" at  $-90^\circ\text{C}$ . The shift difference was of the order of  $\Delta\delta$   $-0.1$  ppm over the  $+50^\circ$  to  $-90^\circ\text{C}$  extremes. A reversed trend of the same magnitude occurred with the peak from H2 (downfield shift upon cooling) whereas the peaks from  $\text{NCH}_2\text{O}$  and  $\text{NCH}_3$  remained at essentially constant shift values. The multiplet ( $50^\circ\text{C}$ ), apparent triplet ( $-20^\circ\text{C}$ ), and "broad singlet" ( $-90^\circ\text{C}$ ) resonance peaks from the lower field hydroxymethylene protons also remained at an essentially constant frequency.

These results are compatible with relatively rapid and conformationally unrestrained motion of the (2-hydroxyethoxy)methyl side-chain. The greater upfield shifting of the oxymethylene proton peak relative to that of the hydroxymethylene proton peak upon cooling is consistent with an extended conformation of the side-chain. In the less hindered region perpendicular to the imidazole ring, the oxymethylene protons might preferentially populate the shielding ring current cone. However, the small shift magnitudes do not offer convincing support.

Treatment of 3 with acetic anhydride in pyridine resulted in formation of two more rapidly migrating (TLC) products. Silica column chromatography effected separation of the two diacetylated derivatives. The more rapidly migrating isomer had  $^1\text{H}$  nmr data consistent with acetylation of the hydroxyl and carbamoyl nitrogen functions. Three-proton NAc and OAc singlets and a three-proton doublet ( $\text{NHCH}_3$ ) were accompanied by two broad NH signals, sharp singlets for the H2 and  $\text{NCH}_2\text{O}$  protons, and two apparent triplets ( $\text{OCH}_2\text{CH}_2\text{O}$ ). No molecular ion peak for this diacetyl compound was observed and its treatment with methanolic ammonia at room temperature resulted in

regeneration of starting **3**. These results are in harmony with its assignment as 4-(N-acetyl-carbamoyl)-1-[(2-hydroxyethoxy)methyl]-5-(methylamino)imidazole (**4**). The ultraviolet spectra of **4** were similar to those of **3**.

The less rapidly migrating diacetyl derivative had <sup>1</sup>H nmr three-proton singlets for NAc, OAc, and NCH<sub>3</sub>, a sharp singlet for H<sub>2</sub>, and two well-separated singlets for the carbamoyl HNH protons. Apparent quartet and triplet resonances were present for the OCH<sub>2</sub>CH<sub>2</sub>OAc AA'BB' protons, respectively, and the NCH<sub>2</sub>O methylene protons appeared as an apparent doublet with the lower intensity side-bands of an AA' system. A molecular ion peak for a diacetyl derivative was present in the mass spectrum of this compound in harmony with its assignment as 5-(N-acetyl-N-methylamino)-1-[(2-acetyloxyethoxy)methyl]-4-carbamoylimidazole (**5**).

Treatment of **5** with methanolic ammonia resulted in deacetylation of the hydroxyl oxygen, only, to give 5-(N-acetyl-N-methylamino)-4-carbamoyl-1-[(2-hydroxyethoxy)methyl]imidazole (**6**). The <sup>1</sup>H nmr spectrum of **6** had three-proton singlets for the NAc and NCH<sub>3</sub> groups plus a sharp singlet for H<sub>2</sub> and two well-separated singlets for the carbamoyl HNH protons. A complex four-proton AA'BB' multiplet for the OCH<sub>2</sub>CH<sub>2</sub>O protons and a clean triplet for the OH proton were present. A narrowly split apparent doublet with the low intensity AA' side-bands from the chemically nonequivalent NCH<sub>2</sub>O protons was again present in this 5-N-acetylated product.

Further evidence for the conjugative donation of lone-pair electrons from the 5-NHCH<sub>3</sub> enamine system in **3** was provided by uv spectral data. The uv spectra of compounds **3** and **4** had shoulders at 270-275 nm and maxima at 256 nm in acid solutions and maxima at 273 nm in aqueous base. In contrast, the uv maxima of the 5-N-acetylated derivatives **5** and **6** were shifted hypsochromically into the vacuum uv region. Only shoulder inflections at ~230 nm were observed.

Compound **3** and its 5-amino (desmethyl) analogue were tested in the viral-infected, neoplastic, and normal control cell culture systems described in ref. 12. Neither compound showed any inhibitory or cytotoxic activity at the highest concentrations examined. Since the favored conformation of the 4-carbamoyl function of **3** has the NH<sub>2</sub> rather than the carbonyl oxygen in the orientation anti to the 4,5-bond of the imidazole ring, it may be "recognized" by thymidine kinases as an adenine-type rather than the acceptable guanine-type analogue. Evaluation of an anti-4-carbonylimidazole analogue remains an interesting question.

#### EXPERIMENTAL

Evaporations were performed at or below room temperature under water aspirator or mechanical oil pump vacuum. Merck silica on plastic sheets (no. 5735) was used for thin-layer chromatography (TLC) with uv detection of products under a 2537 Å lamp. Column chromatography was conducted with Merck silica (no. 7734, 63-200 μm). NMR spectra were determined under ambient operating

conditions with  $(\text{CD}_3)_2\text{SO}$  as solvent unless otherwise specified.

9-[(2-Hydroxyethoxy)methyl]-3-methyl-6-(dimethylamino)purine Iodide (2). A solution of 1.0 g (4.2 mmol) of 9-[(2-hydroxyethoxy)methyl]-6-(dimethylamino)purine (1) and 2 ml (32 mmol) of methyl iodide in 5 ml of DMF was allowed to stand for 3 weeks at  $-0^\circ\text{C}$  (refrigerator). The resulting crystals were collected by filtration and washed with acetone to give 882 mg (55%) of 2: mp  $238-242^\circ\text{C}$  dec;  $^1\text{H}$  nmr (100 MHz)  $\delta$  3.40 and 3.87 (s and s, 3 and 3,  $\text{N}(\text{CH}_3)_2$ ), 3.51 (br s, 4,  $\text{OCH}_2\text{CH}_2\text{O}$ ), 4.23 (s, 3,  $\text{NCH}_3$ ), 5.91 (s, 2,  $\text{NCH}_2\text{O}$ ), 8.61 and 8.72 (s and s, 1 and 1, H8 and H2); MS (FAB/glycerol)  $m/z$  252 ( $\text{M}^+ - \text{I}^-$ ); uv (0.1N  $\text{HCl}/\text{H}_2\text{O}$ ) max 286 nm ( $\epsilon$  18,200), min 247 nm ( $\epsilon$  3900). Anal. Calcd. for  $\text{C}_{11}\text{H}_{18}\text{N}_6\text{O}_2$ : C, 34.84; H, 4.78; N, 18.47. Found: C, 34.83; H, 4.89; N, 18.47.

4-Carbamoyl-1-[(2-hydroxyethoxy)methyl]-5-(methylamino)imidazole (3). A solution of 900 mg (2.37 mmol) of 2 in 18 ml of 50% 2N  $\text{KOH}/\text{H}_2\text{O}/\text{EtOH}$  was heated at reflux for 1 h. The cooled solution was neutralized with Amberlite IR-120( $\text{H}^+$ ) resin, filtered, and evaporated. The residue was chromatographed on a short column of silica gel (25 g) with 20%  $\text{EtOH}/\text{CHCl}_3$ . Appropriate fractions were pooled, evaporated, and the residue was crystallized from 95%  $\text{EtOH}$  to give 418 mg (82%) of 3: mp  $124.5-126^\circ\text{C}$ ;  $^1\text{H}$  nmr (400 MHz)  $\delta$  2.92 (d,  $J = 6$  Hz, 3,  $\text{NCH}_3$ ), 3.49 (m, 4,  $\text{OCH}_2\text{CH}_2\text{O}$ ), 4.70 (t,  $J = 5$  Hz, 1, OH), 5.33 (s, 2,  $\text{NCH}_2\text{O}$ ), 6.05 (q,  $J = 6$  Hz, 1,  $\text{NHCH}_3$ ), 6.79 and 6.95 (s and s, 1 and 1,  $\text{CONH}_2$ ), 7.35 (s, 1, H2); MS  $m/z$  214.1067 (calcd. for  $\text{M}^+$ : 214.1066); uv (0.1N  $\text{HCl}/\text{H}_2\text{O}$ ) shoulder 270 nm ( $\epsilon$  7600), max 256 nm ( $\epsilon$  8200), min 225 nm ( $\epsilon$  3300), (0.1N  $\text{NaOH}/\text{H}_2\text{O}$ ) max 273 nm ( $\epsilon$  9400), min 228 nm ( $\epsilon$  5000). Anal. Calcd. for  $\text{C}_8\text{H}_{14}\text{N}_4\text{O}_3$ : C, 44.85; H, 6.59; N, 26.15. Found: C, 44.63; H, 6.65; N, 26.27.

Acetylation of 3. A solution of 600 mg (2.8 mmol) of 3 in 5 ml of pyridine was cooled to  $0^\circ\text{C}$  and treated with 600 mg (5.9 mmol) of  $\text{Ac}_2\text{O}$ . After 2 h, complete disappearance of 3 had occurred and two more rapidly migrating (TLC, 10%  $\text{MeOH}/\text{CHCl}_3$ ) products were observed. Evaporation of volatiles followed by column chromatography (100 g of silica gel, 5%  $\text{MeOH}/\text{CHCl}_3$ ) gave 250 mg (30%) of the more rapidly migrating product which was crystallized from  $\text{CHCl}_3/\text{PhCH}_3$  to give 4-(N-acetylcabamoyl)-1-[(2-acetyloxyethoxy)methyl]-5-(methylamino)imidazole (4): mp  $88.5-91^\circ\text{C}$ ;  $^1\text{H}$  nmr ( $\text{CDCl}_3$ , 200 MHz)  $\delta$  1.66 (s, 3,  $\text{NAc}$ ), 2.08 (s, 3,  $\text{OAc}$ ), 3.01 (d,  $J = 6$  Hz, 3,  $\text{NCH}_3$ ), 3.70 and 4.24 (AA'BB' m, 2 and 2,  $\text{OCH}_2\text{CH}_2\text{OAc}$ ), 5.31 (s, 2,  $\text{NCH}_2\text{O}$ ), 5.99 (br s, 1,  $\text{NHCH}_3$ ), 6.55 (br s, 1,  $\text{CONHAc}$ ), 7.10 (s, 1, H2); uv (0.1N  $\text{HCl}/\text{H}_2\text{O}$ ) shoulder 274 nm, max 256 nm, min 226 nm (0.1N  $\text{NaOH}/\text{H}_2\text{O}$ ) max 273 nm, min <220 nm, (MeOH) max 274 nm, min 216 nm.

The less rapidly migrating product was crystallized from  $\text{MeOH}/\text{PhCH}_3$  to give 203 mg (24%) of 5-(N-acetyl-N-methylamino)-1-[(2-acetyloxyethoxy)methyl]-4-carbamoylimidazole (5): mp  $184-186^\circ\text{C}$ ;  $^1\text{H}$  nmr (400 MHz)  $\delta$  1.69 (s, 3,  $\text{NAc}$ ), 1.96 (s, 3,  $\text{OAc}$ ), 3.00 (s, 3,  $\text{NCH}_3$ ), 3.65 ("q", 2,  $\text{OCH}_2$ ), 4.10 ("t", 2,  $\text{CH}_2\text{OAc}$ ), 5.29 ("d", 2,  $\text{NCH}_2\text{O}$ ), 7.25 and 7.42 (s and s, 1 and 1,  $\text{CONH}_2$ ), 6.98 (s, 1, H2);

MS  $m/z$  298.1278 (calcd. for  $M^+$ : 298.1277); uv (0.1N HCl/H<sub>2</sub>O) and (MeOH) shoulder ~228 nm (0.1N NaOH/H<sub>2</sub>O) shoulder ~230 nm.

5-(N-Acetyl-N-methylamino)-4-carbamoyl-1-[(2-hydroxyethoxy)methyl]imidazole (6). A 150-mg (0.5 mmol) sample of 5 was treated with 10 ml of NH<sub>3</sub>/MeOH (saturated at 0°C) at room temperature overnight. Evaporation of volatiles and crystallization of the residue from MeOH gave 104 mg (81%) of 6: mp 170-172°C; <sup>1</sup>H nmr (400 MHz) δ 1.70 (s, 3, NAc), 3.01 (s, 3, NCH<sub>3</sub>), 3.46 (AA'BB' m, 4, OCH<sub>2</sub>CH<sub>2</sub>O), 4.72 (t, J = 5 Hz, 1, OH), 5.28 ("d", 2, NCH<sub>2</sub>O), 7.23 and 7.41 (s and s, 1 and 1, CONH<sub>2</sub>), 7.96 (s, 1, H<sub>2</sub>); MS  $m/z$  256.1174 (calcd. for  $M^+$ : 256.1172); uv (0.1N HCl/H<sub>2</sub>O) and (MeOH) shoulder ~228 nm (ε 9800), (0.1N NaOH/H<sub>2</sub>O) shoulder ~232 nm (ε 9900). Anal. Calcd. for C<sub>16</sub>H<sub>16</sub>N<sub>4</sub>O<sub>4</sub>: C, 46.87; H, 6.29; N, 21.86. Found: C, 46.60; H, 6.24; N, 21.82.

X-Ray Analysis of 3. Precession photographs of a colorless crystal, measuring 0.4 x 0.4 x 0.1 mm, showed systematic absences corresponding to space groups Pca2<sub>1</sub> or Pbcm. In view of the absence of chiral centers and the presence of eight molecules in the unit cell, the latter space group was chosen for data collection. The crystal was mounted on a CAD4 diffractometer and the following data were obtained:

Orthorhombic, a = 8.718(1), b = 18.351(2), c = 12.570(2) Å, v = 2011.0 Å<sup>3</sup>, ρ<sub>c</sub> = 1.42 g cm<sup>-3</sup>, Z = 8 (20°C, CuKα<sub>1</sub>, λ = 1.54056 Å), F(000) = 912, μ(CuKα) = 8.86 cm<sup>-1</sup>.

Unit cell parameters were determined from a least-squares refinement of 22 high-order (41° < θ < 54°) reflections. Intensities were measured with Ni-filtered CuKα radiation, using ω/2θ scans with variable scan ranges and speeds. Two standard reflections were monitored at regular intervals; their intensities fluctuated by ±3% during the data collection. There were 2187 unique reflections with 2θ ≤ 152° of which 74 with I < 3σ(I) were considered unobserved. The intensities were corrected for Lorentz and polarization factors; absorption corrections were considered unnecessary.

The statistics of E values clearly indicated an acentric space group which had to be Pca2<sub>1</sub> (no. 29) with two molecules in the asymmetric unit. In order to avoid re-indexing of all reflections, the alternative space group Pbc2<sub>1</sub> was chosen which has the following equivalent positions: x, y, z; x̄, ȳ, ½z̄; x, ½ȳ, ½z̄; x̄, ½y, z. The structure was determined by direct methods with the aid of the computer program MULTAN78.<sup>25</sup> Of the 20 starting sets subjected to tangent refinement, the solution with the highest combined figure of merit yielded an E map on which all 30 atoms in the asymmetric unit could be located. Refinement was carried out by the block-diagonal least-squares procedure. Anisotropic temperature parameters were used for nonhydrogen atoms, while hydrogen atoms, located on difference Fourier maps, were refined with isotropic parameters. The scattering factors were taken from the International Tables for X-Ray Crystallography<sup>26</sup> and the oxygen curve was corrected for anomalous dispersion. Throughout the refinement the function

Table 3. Final atomic coordinates and thermal parameters.<sup>a</sup>

Atom	$\underline{x/a}$	$\underline{y/b}$	$\underline{z/c}$	$\underline{U_{eq}}$
N1A	10478(2)	2714(1)	6608(2)	372
C2A	10803(3)	2620(1)	7669(2)	410
N3A	10244(3)	2022(1)	8045(2)	402
C4A	9470(3)	1689(1)	7197(2)	349
C5A	9611(3)	2120(1)	6285(2)	352
C6A	8618(3)	1017(1)	7385(2)	382
N7A	8812(4)	718(1)	8347(2)	493
O8A	7748(3)	737(1)	6717(1)	526
N9A	9113(3)	2085(1)	5261(2)	468
C10A	8933(5)	1404(2)	4694(3)	562
C1'A	11026(3)	3303(1)	5933(3)	432
C4'A	9377(5)	4237(2)	6548(3)	539
O4'A	9861(2)	3798(1)	5663(2)	434
C5'A	8425(4)	4858(2)	6144(3)	565
O5'A	7016(3)	4599(2)	5805(3)	711
N1B	5457(2)	2520(1)	4291(2)	408
C2B	6190(4)	2426(2)	3333(3)	483
N3B	5716(3)	1855(1)	2818(2)	454
C4B	4582(3)	1558(1)	3457(2)	387
C5B	4421(3)	1961(1)	4375(2)	377
C6B	3741(3)	896(1)	3189(2)	401
N7B	4164(4)	541(1)	2322(2)	528
O8B	2658(3)	683(1)	3758(2)	534
N9B	3372(3)	1848(2)	5178(2)	503
C10B	3884(6)	1837(3)	6274(3)	720
C1'B	5711(4)	3137(2)	5012(3)	495
C4'B	4249(5)	4043(2)	4114(3)	623
O4'B	4462(3)	3613(1)	5043(2)	514
C5'B	3310(5)	4707(2)	4397(3)	623
O5'B	4185(3)	5180(1)	5048(3)	680

<sup>a</sup>All values were multiplied by 10<sup>4</sup>.

$\sum_w \left( \left| \frac{F_o}{F_c} \right| - \left| \frac{F_o}{F_c} \right| \right)^2$  was minimized and a factor of 0.8 was applied to all shifts. The following weighting scheme was used during the final stages:  $w = w_1 \cdot w_2$ , where  $w_1 = 1$  for  $\left| \frac{F_o}{F_c} \right| < 8$ ,  $w_1 = 8 / \left| \frac{F_o}{F_c} \right|$  for  $\left| \frac{F_o}{F_c} \right| \geq 7$ ,  $w_2 = \sin^2 \theta / 0.7$  for  $\left| \frac{F_o}{F_c} \right| \leq 0.7$ ,  $w_2 = 1$  for  $\left| \frac{F_o}{F_c} \right| > 0.7$ . This scheme made the average values of  $w(\Delta F^2)$  independent of  $\left| \frac{F_o}{F_c} \right|$  and  $\sin^2 \theta$ . After the final cycle the average parameter shift equalled  $0.2\sigma$  and the largest one  $1.0\sigma$ . A final difference Fourier map showed no significant features. Three strong, low-order reflections suffered from secondary extinction effects and were given zero weights. The final conventional residual index  $R$  is 0.048 and the weighted index  $R_w$  is 0.058 for 2110 observed reflections. Final atomic parameters are listed in Table 3.

## ACKNOWLEDGEMENTS

Apart from MULTAN78,<sup>25</sup> all crystallographic computations were carried out with programs written by Ahmed et al.<sup>27</sup> Figure 1 was drawn with the ORTEP program of Johnson.<sup>28</sup> Financial support was provided, in part, by the Natural Sciences and Engineering Research Council of Canada, the National Cancer Institute of Canada, and an Alberta Heritage Foundation for Medical Research Fellowship to P.W.H.

## REFERENCES AND NOTES

1. NRCC No. 25828; Nucleic Acid Related Compounds. 50. For the previous paper in this series see: F. Hansske and M.J. Robins, Tetrahedron Lett., 1985, 26, 4295.
2. To whom inquiries on X-ray crystallography should be sent.
3. To whom other inquiries should be sent.
4. G.B. Elion, P.A. Furman, J.A. Fyfe, P. de Miranda, L. Beauchamp, and H.J. Schaeffer, Proc. Natl. Acad. Sci. U.S.A., 1977, 74, 5716.
5. J.A. Fyfe, P.M. Keller, P.A. Furman, R.L. Miller, and G.B. Elion, J. Biol. Chem., 1978, 253, 8721.
6. D. Derse, Y.-C. Cheng, P.A. Furman, M.H. St. Clair, and G.B. Elion, J. Biol. Chem., 1981, 256, 11447.
7. P.A. Furman, M.H. St. Clair, and T. Spector, J. Biol. Chem., 1984, 259, 9575.
8. L.B. Townsend, Chem. Rev., 1967, 67, 533.
9. A. Parkin and M.R. Harnden, J. Heterocycl. Chem., 1982, 19, 33.
10. T. Itaya, H. Matsumoto, and T. Watanabe, Chem. Pharm. Bull., 1982, 30, 86.
11. M.J. Robins and P.W. Hatfield, Can. J. Chem., 1982, 60, 547.
12. M.J. Robins, P.W. Hatfield, J. Balzarini, and E. De Clercq, J. Med. Chem., 1984, 27, 1486.
13. T. Saito and T. Fujii, J. Chem. Soc., Chem. Commun., 1979, 135.

14. K. Nielsen and I. Søjtofte, Acta Chem. Scand. Ser. A, 1985, 39, 259.
15. R.K. McMullan, J. Epstein, J.R. Ruble, and B.M. Craven, Acta Crystallogr. Sect. B, 1979, 35, 688.
16. K. Simon, J. Schwartz, and A. Kálmán, Acta Crystallogr. Sect. B, 1980, 36, 2323.
17. D.A. Adamiak and W. Saenger, Acta Crystallogr. Sect. B, 1979, 35, 924.
18. H.C. Freeman and N.D. Hutchinson, Acta Crystallogr. Sect. B, 1979, 35, 2051.
19. M. Burke-Laing and M. Laing, Acta Crystallogr. Sect. B, 1976, 32, 3216.
20. The excess bond order over 7.00 can be ascribed to the sp<sup>3</sup>, rather than sp<sup>2</sup>, hybridization of N1.<sup>19</sup>
21. G.I. Birnbaum, M. Cygler, and D. Shugar, Can. J. Chem., 1984, 62, 2646.
22. G.I. Birnbaum and D. Shugar, 'Topics in Nucleic Acid Structure', ed. by S. Neidle, Macmillan, London, in press.
23. S. Wolfe, Acc. Chem. Res., 1972, 5, 102.
24. G.I. Birnbaum, R. Stolarski, Z. Kazimierczuk, and D. Shugar, Can. J. Chem., 1985, 63, 1215.
25. P. Main, S.E. Hull, L. Lessinger, G. Germain, J.P. Declercq, and M.M. Wolfson, MULTAN78, University of York, England, and University of Louvain, Belgium, 1978.
26. 'International Tables for X-ray Crystallography', Vol. IV, Kynoch Press, Birmingham, 1974.
27. F.R. Ahmed, S.R. Hall, M.E. Pippy, and C.P. Huber, J. Appl. Crystallogr., 1973, 6, 309.
28. C.K. Johnson, ORTEP II Report ORNL-5138, Oak Ridge National Laboratory, Oak Ridge, TN, 1976.

Received, 2nd June, 1986